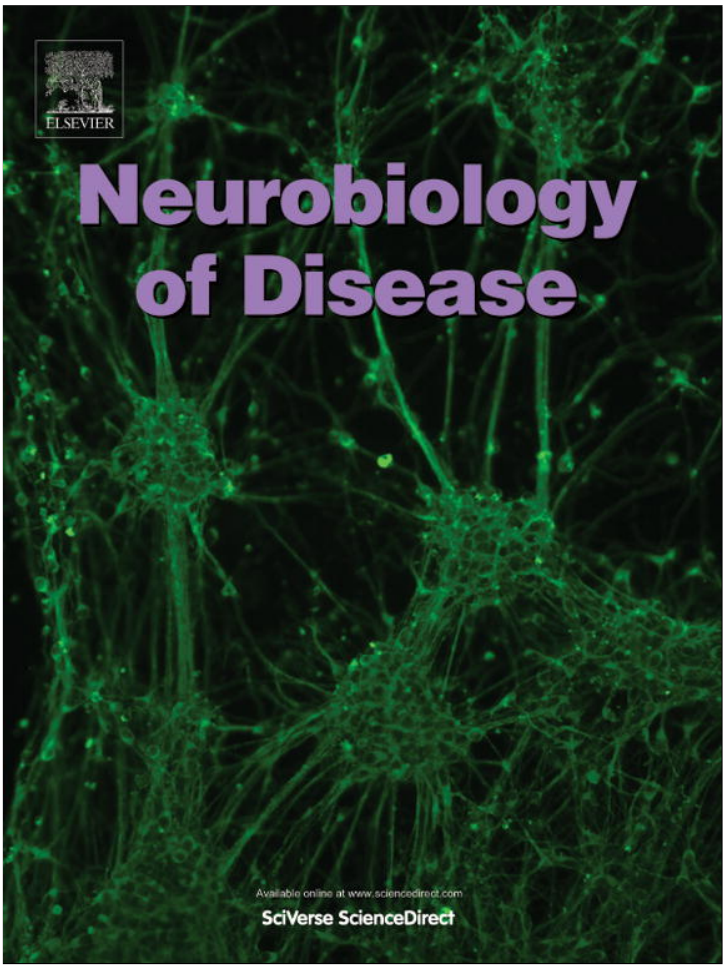

(This is a sample cover image for this issue. The actual cover is not yet available at this time.)

Neurobiology of Disease 48 (2012) 317–328

Contents lists available at SciVerse ScienceDirect

Neurobiology of Disease

journal homepage: www.elsevier.com/locate/ynbdi

The loss of interneuron functional diversity in the piriform cortex after induction of experimental epilepsy

Cezar Gavrilovici, Emily Pollock, Michelle Everest, Michael O. Poulter *

Molecular Brain Research Group, Robarts Research Institute, Department of Physiology and Pharmacology, University of Western Ontario, London, Ontario, Canada N6A 5K8

ARTICLE INFO

Article history:
Received 25 May 2012
Revised 28 June 2012
Accepted 5 July 2012
Available online 16 July 2012

Keywords:
Experimental epilepsy
Interneuron
Kv 1.6
Piriform cortex
Firing pattern

ABSTRACT

Interneuronal functional diversity is thought to be an important factor in the control of neural network oscillations in many brain regions. Specifically, interneuron action potential firing patterns are thought to modulate brain rhythms. In neurological disorders such as epilepsy where brain rhythms are significantly disturbed interneuron function is largely unexplored. Thus the purpose of this study was to examine the functional diversity of piriform cortex interneurons (PC; an area of the brain that easily supports seizures) before and after kindling-induced epilepsy. Using cluster analysis, we found five control firing behaviors. These groups were termed: non-adapting very high frequency (NAvHF), adapting high frequency (AHF), adapting low frequency (ALF), strongly adapting low frequency (sALF), and weakly adapting low frequency (wALF). A morphological analysis showed these spiking patterns were not associated with any specific interneuronal morphology although we found that most of the cells displaying NAvHF firing pattern were multipolar. After kindling about 40% of interneuronal firing pattern changed, and neither the NAvHF nor the wALF phenotypes were found. We also found that in multipolar interneurons a long-lasting potassium current was increased. A qPCR analysis indicated Kv1.6 subtype was up-regulated after kindling. An immunocytochemical analysis showed that Kv1.6 protein expression on parvalbumin (multipolar) interneurons increased by greater than 400%. We also examined whether these changes could be due to the selective death of a subset of interneurons but found that there was no change in cell number. These data show an important loss of the functional diversity of interneurons in the PC. Our data suggest that under pathophysiological condition interneurons are plastic resulting in the attenuation of high frequency network oscillations in favor of low frequency network activity. This may be an important new mechanism by which network synchrony is disturbed in epileptic seizures.

Introduction

The piriform cortex (PC) is a three layered phylogenetically old cortical structure (paleocortex) that is part of the limbic system. In addition to olfactory sensation and memory processing (Haberly, 2001), the PC has also been implicated in the development of seizures (Loscher and Ebert, 1996; Racine et al., 1988). As in all cortical networks, the GABAergic interneuron system within the PC is important for the regulation of neuronal excitability and rhythmicity of the neural network, participating in both feed-forward and feedback inhibitory loops (Haberly, 1983; Kelly et al., 2002; Neville and Haberly, 2004). These circuits have been shown to modulate associative long-term potentiation (Kanter and Haberly, 1993) and generate oscillatory activities in the PC (Neville and Haberly, 2003). It has also been shown that the PC is a heterogeneous structure with anatomical differences along the rostro-caudal axis, including differences in layer thickness (Haberly and Price, 1978), the number of interneurons per layers (Haberly et al., 1987; Loscher et al., 1998) as well differences in the laminar distribution/orientation of associational fibers (Haberly and Price, 1978; Luskin and Price, 1983). These morphological traits are thought to reflect different functional roles along the anterior–posterior axis of the PC (Neville and Haberly, 2004). In light of this diverse functionality, the focus on morphological and electrophysiological characteristics of interneuronal subpopulations in the PC has increased. A recent study by Suzuki and Bekkers (2010) has demonstrated in mouse PC a variety of interneuron firing patterns that are similar in many ways to those found in other limbic regions. These included those that fired at high (>50 Hz) and low (<50 Hz) frequencies and those that fired at a constant (non-adapting) or decreasing (adapting) rate. The role of these interneuron firing patterns in the PC has not been examined in the detail that various firing patterns have been studied in other brain regions such as the hippocampus and neocortex.

Additionally, whether these firing patterns are amenable to change in response to either physiological or pathophysiological stimuli has yet to be explored. Given the intimate roles or "subdivision of labor" (Klausberger and Somogyi, 2008) that these neurons

* Corresponding author at: Molecular Brain Research Group, Robarts Research Institute, Department of Physiology and Pharmacology, University of Western Ontario, London, Ontario, Canada N6A 5K8.
E-mail address: mpoulter@robarts.ca (M.O. Poulter).
Available online on ScienceDirect (www.sciencedirect.com).

0969-9961/$ – see front matter © 2012 Elsevier Inc. All rights reserved.
doi:10.1016/j.nbd.2012.07.002

seem to control with regard to defining differing oscillatory patterns in neural circuits, disturbances in their firing patterns may have wide ranging effects on behavior. Here we have investigated the hypothesis that in the kindling model of epilepsy interneuron firing patterns may be disturbed. We found that in contrast to control tissue, kindled neurons lose the non-adapting phenotype and the ability to fire at very high frequencies (>100 Hz). This change was not accounted for by cell death but rather an increase in the expression of the Kv1.6 subtype of potassium channels on multipolar interneurons which normally are capable of firing at very high frequency non-adapting rates. Our observations indicate that there is a loss of interneuron firing diversity in the PC after the induction of kindled induced epileptic seizures.

Materials and methods

Adult male Sprague Dawley rats (Charles River), weighing 200–250 g at the time of the study (n = 45), were used. All experiments were conducted in accordance with the guidelines of the Canadian Council on Animal Care and protocols approved by The University of Western Ontario Animal Care Committee.

Electrode implantation

Animals (n = 20) were anesthetized with Ketamine–Dormitor mixture (0.1 ml/100 g; i.p.) and implanted with two bipolar stimulating/recording electrodes bilaterally in the basolateral amygdala (BLA) with the following coordinates: 2.6 mm posterior to Bregma, 4.5 mm lateral to midline and 8.0 mm ventral (Paxinos and Watson, 1986). Post-mortem histological confirmation of intracranial location of electrodes in BLA was performed for all kindled rats.

The electrodes were constructed of two twisted strands of 0.127-mm diameter Diamel-insulated Nichrome wire and were attached to male Amphenol pins. The electrodes were implanted and secured to the skull with jeweler's screws. The electrode assembly was fixed to the skull by dental acrylic cement (McIntyre and Molino, 1972).

Kindling protocol

The kindling protocol began 1 week after the surgery. The afterdischarge threshold (ADT) was determined in each amygdala by delivering a 2-s 60-Hz sine wave stimulus of progressively increasing intensity (delivered once every minute at 15, 25, 35, 50, 75, 100,150, 200, 250, 300 and 350 μA) until an ADT was triggered (Gavrilovici et al., 2006; McIntyre and Plant, 1993). The rats were stimulated daily until six generalized stage 5 convulsions on the Racine's scale were elicited. Seizure severity and duration were recorded daily during the kindling acquisition. Fully kindled rats were allowed to recover for a minimum of 2 weeks (range 2–3 weeks) after the last seizure (Gavrilovici et al., 2006; McIntyre and Plant, 1993).

Tissue preservation, slicing procedures and maintenance

Coronal rat brain slices (350 μm; 1.5 to −0.3 mm relative to Bregma) were performed according to published methodology (Gavrilovici et al., 2006; McIntyre et al., 2002a). The anesthetized rats (Ketamine–Dormitor mixture; 0.1 ml/100 g; i.p.) were perfused through the heart with an ice-cold Ringer solution in which sodium was replaced by choline [containing (in mM): Choline Cl 110, KCl 2.5, NaH_2PO_4 1.2, $NaHCO_3$ 25, $CaCl_2$ 0.5, $MgCl_2$ 7, Na pyruvate 2.4, ascorbate 1.3, dextrose 20] as previously described (Gavrilovici et al., 2006; McIntyre et al., 2002a). After heart perfusion, the brain was removed and temporal lobe was coronally sliced using a Vibratome. The slices were incubated at 37 °C for 30 min and subsequently moved to a room-temperature (22 °C) bath for at least 45 min. Slicing, incubation, and storage were all performed in the choline solution (see above). The Ringer's solution used during electrical recordings was similar to the choline solution except pyruvate and ascorbate were removed, equimolar NaCl replaced the choline Cl, and $CaCl_2$ and $MgCl_2$ were both used at a 2 mM concentration (McIntyre et al., 2002a). All solutions were maintained at pH 7.4 and bubbled with 5%CO2/95%O_2 (carbogen).

Electrophysiology

Patch electrodes were pulled from borosilicate glass capillaries and filled with K^+-gluconate solution having a composition (in mM) of: potassium gluconate 147, KCl 1, $CaCl_2$ 2, HEPES 10, EGTA 10, Glucose 10, MgATP 2, and GTP 0.3 (300 mOsm, pH 7.3–7.4). As this electrode solution has been shown to potentially block some potassium currents in hippocampus we also used an internal solution containing K^+ methanesulfonate (n = 34) to check that the identified spiking patterns were not influenced by the K^+ gluconate based internal solution (Zhang et al., 1994). These recordings were indistinguishable from control recordings. The K^+ methanesulfonate solution was not used throughout this study as we found that the cells did not support this internal solution as effectively as when the K^+ gluconate solution was employed. Whole-cell patch clamp recordings from neurons in layers 1–3 of anterior PC were made with an EPC 9/2 amplifier (HEKA, Lambrecht, Germany). Series resistance compensations were performed in all recordings. The initial access was <20 MΩ and compensated by 50–70%. All experiments were performed at 32 °C. Voltage-gated currents and excitability of the cell were monitored by means of voltage-clamp and current-clamp protocols (PulseFit v 8.0; Heka, Germany). Cell responses were obtained in less than 5 min after forming whole-cell configuration by injecting hyperpolarizing and depolarizing current steps (500 ms pulse; 50 pA increments). Input resistance (R_I) was calculated by linear regression of the current–voltage relationship in response to hyperpolarizing steps (as described in Dietrich et al., 2005) using Origin software (Microcal, Northampton, MA). Firing pattern analysis was performed at the current level that produced reliable repetitive firing (twice the firing threshold), in the presence of NMDA, AMPA and kainate channel blockers (20 μm 2-amino phosphonovaleric acid, APV and 10 μm dinitroquinoxaline-2,3-dione, DNQX; Research Biochemicals, Natick, MA, USA). Interspike interval ratio (II_R) was obtained by dividing the last interspike interval (measured in milliseconds) by the duration of the first interval, as described in Kroner et al. (2007). In a small number of recordings (n = 25) blocking $GABA_A$ receptors with gabazine (10 μM; added to the perfusion bath) did not affect the interneuron firing pattern in kindled animals. The effect of gabazine (10 μM) on GABAergic current (n = 9) was tested in the presence of sodium, NMDA, AMPA and kainate channel blockers, using a KCl electrode solution (as described in Gavrilovici et al., 2006).

Also, in a number of recordings (n = 72) to evaluate the K^+ current, before and after kindling, sodium and calcium channel blockers (250 nM TTX, and 1 mM $NiCl_2$) were added into the bath perfusion. Potassium outward currents were evoked by depolarizing steps between −50 and +10 mV, leak-subtracted and measured at the end of each pulse (PulseFit v 8.0; Heka, Germany).

Finally, a small number of current clamp recordings (n = 15) were performed on sham rats (electrode implanted, but never kindled) of the same age as kindled and control group rats, using identical protocols. The five firing patterns were observed in the sham rats (NAvHF, AHF, ALF, sALF and wALF), and corresponded to the firing patterns seen in control rats.

Cluster analysis

Unsupervised cluster analysis was performed on interneuronal populations of PC using Ward's method with *z*-score normalization and intervals calculated by Euclidian squared distances (SPSS 13, Chicago, Illinois, USA) according to described methodology (Cauli et al., 2000). The analysis was based on their main electrophysiological

parameters: input resistance, firing frequency and interspike interval ratio, providing five distinct firing groups. Comparisons among different firing pattern groups were made by using ANOVA and a Tukey multiple comparison post-hoc test as appropriate. All data are presented as means ± standard error of the mean. The naming of the five phenotypes identified by the cluster analysis was done according to the terminology described by Kroner et al. (2007) and Ascoli et al. (2008). Specifically, neurons with $II_R < 1.25$ were grouped as non-adapting cells while neurons with $II_R > 1.25$ were classified as adapting cells. Those with an average firing frequency (FF) > 50 Hz were termed as high frequency while those FF < 50 Hz were termed as low frequency.

Histochemistry

In order to reconstruct the morphology and understand where the recordings were made, patch electrodes included 0.2% Biocytin. After the completion of a recording, the slice was removed from the microscope chamber and fixed in paraformaldehyde solution (4% paraformaldehyde in 0.1 phosphate buffer) for 5–7 days. The sections were washed for 15 min in PBS followed by a 30 min rinse in PBS-TX and 90 min incubation in streptavidin-conjugated Alexa Fluor-594 (5 μg/ml; Molecular Probes) at room temperature. After rinsing in PB-TX for 30 min, the slices were mounted on slides for viewing on a confocal microscope.

Image acquisition and morphological reconstruction of patched neurons

Confocal images were taken on an Olympus IX 60 inverted microscope outfitted with a Perkin Elmer Spinning Disk Confocal attachment with a 20× (N.A. = 0.50) objective. The microscope was equipped with a Hamamatsu Orca ER CCD camera (1300×1030 pixels), and images were acquired in Volocity software (Improvision, Lexington, MA). Each image represents a stack of 40–50 images 0.2 μm apart in the z-plane. For morphological reconstruction of the dendritic arborization of patched neurons, the stacks of confocal images were deconvolved with Auto-Quant software (Auto quant X2, Media Cybernetics, Bethesda, MD) and then processed with Imaris Filament Tracer module in "Surpass mode" (Bitplane, Zurich, Switzerland). Filament tracer creates dendritic arborization patterns based on an algorithm that predicts arborization pathways. These pathways are set up by the user-set criteria of a start point, namely, the size of cell somata, and an end point representing minimum thickness of processes. Start points were set to 10 μm, and endpoints were set to 1 μm. The resultant filament lines were converted from lines to two-pixel-thick cones. To mark the cell bodies, an "Isosurface" was then created. This process creates a cell body from the stack of images that is then merged with the dendritic morphology (see Gavrilovici et al., 2010).

We used the criteria for classification of pyramidal versus non-pyramidal cells as previously described (Gavrilovici et al., 2006; McIntyre et al., 2002a) and were based on: 1) soma morphology; 2) axonal projection to deeper layers for pyramidal cells; 3) presence of dendritic spines for pyramidal cells; and 4) spiking properties. A few cells that were spiny non-pyramidal were also found but not included in the analysis. Based on the morphologies that we have previously described (Gavrilovici et al., 2010), interneurons were further grouped into three categories: 1) horizontal cells (usually calbindin immunoreactive; CB-IR) having extended dendrites in the horizontal plane — parallel to the PC layers; 2) multipolar cells (usually parvalbumin; PV-IR or PV-IR/CB-IR) having a round dendritic tree crossing into adjacent layers and 3) vertical/bipolar-bitufted cells (usually calretinin immunoreactive; CR-IR) having extended dendrites in the vertical plane, perpendicular to PC layers. PC layer depth and demarcation between adjacent layers were set according to Ekstrand et al. (2001) and Neville and Haberly (2004). This analysis does not include neurogliaform neurons as they are rare in rat piriform and sufficient numbers of recordings were not obtained to make a valid comparison.

QPCR analysis

The same animals used in the electrophysiology experiments were used as a source of cellular RNA. Tissue not used for electrophysiology was immediately frozen at −80 °C until further use. Micro dissected PC was placed in Trizol (Invitrogen) and homogenized. RNA was extracted from the homogenate following the manufacturer's protocol. RNA purity and quantity were analyzed using a NanoDrop 1000 spectrometer. RNA (2 μg) with a 260/280 above 1.80 was reverse transcribed using the Invitrogen Superscript II protocol with oligo(dT) primers. QPCR reactions were performed in duplicate for each sample using BioRad MyIQ single-color real-time PCR detection system. DNA abundance was detected using SYBR Green (Bio Rad iQ SYBR Green Supermix) following the manufacturer's protocol. An initial screen of more than 80 genes that code for ion channels in the rat nervous system was done using RT^2 Profiler™ rat PCR array (PARN-036, Qiagen). This was done by pooling equal amounts of RNA from 5 control and 5 kindled rat brains. Potassium channel's mRNA abundance that appeared to be increased by one cycle or more was further assessed by analyzing the expression of 11 control and 9 kindled rats individually. For these experiments primers were designed in house. QPCR primer efficiency was quantified using a five point 10× dilution series of rat brain cDNA (100 ng–10 pg). PCR primer sets had between 90 and 110% efficiency at 55 °C annealing. Neuron specific enolase was chosen as a reference gene (Forward: 5′-GGTCCAAGTTCACAGCCAAT-3′, Reverse: 3′-CCTT GAGCAGCAAACAGTTG-5′) to normalize gene expression levels. The following primer sequences for the potassium channel mRNA expression were: Kv2.1 — Forward: 5′-TGAGCTGCAGAGCCTAGA CGAGT-3′, Reverse: 5′-ACCTCAGCAAGTACTCCATGG TGA-3′; Kv9.3 — Forward: 5′-GTGGATCAGAGTACACTCCTGCGG-3′, Reverse: 5′-AGAATGGCCTCCT CAGAG TGGCAG-3′; Kv1.2 — Forward: 5′-ATGACAGTGGCTACCGGAG AC C-3′, Reverse: 5′-TCGTGGTCTGCCTCTGGGTCATA-3′; and Kv1.6 — Forward: 5′-TGTGAGTGGTGGCAG TGGTCAGAA-3′, Reverse: 5′-TGAA GATCCGAAACACCCGGACCA-3′. Differences in abundance are shown as a comparison of the Δ cycle thresholds (C_t) between control and kindled brain samples. ΔC_t is the $C_{t\ (\text{reference gene})} - C_{t\ (\text{gene of interest})}$. The data were statistically analyzed using one-way ANOVA. Data are expressed as mean ± standard error of the ΔC_t values.

Immunocytochemical analysis of potassium channel expression

Tissue preparation and fixation

Rats were deeply anesthetized with Ketamine–Dormitor mixture (0.1 ml/100 g; i.p.) and perfused intracardially with 0.1 M phosphate-buffered saline (PBS), pH 7.3, followed by LANA's solution (4% paraformaldehyde and 20% picric acid in phosphate-buffered saline). The brain was then removed from the skull and left in LANA's solution for further 24 h and then stored in 30% sucrose, 0.1 M phosphate buffer (PB), pH

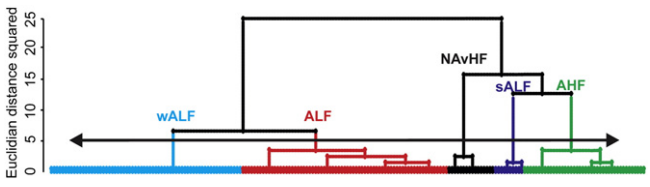

Fig. 1. Cluster analysis of electrophysiological properties of rat piriform cortex interneuronal populations before kindling-induced epilepsy. The x-axis of dendrogram shows individual cells (n = 205) and the y-axis represents the linkage distance measured by Euclidean distance squared. Double arrow solid line represents the cut off showing five distinct clusters: non-adapting very high frequency (NAvHF), adapting high frequency (AHF), adapting low frequency (ALF), strongly adapting low frequency (sALF), and weakly adapting low frequency (wALF).

Table 1
Electrophysiological properties of the five types of interneuronal firing groups in the anterior piriform cortex.

	Cluster 1 ALF (n = 71)	Cluster 2 AHF (n = 42)	Cluster 3 sALF (n = 10)	Cluster 4 wALF (n = 66)	Cluster 5 NAvHF (n = 16)
RMP (mV)	−76.0 ± 0.9	−76.2 ± 1.3	−70.6 ± 2.9	72.7 ± 0.8	−76.0 ± 0.9
R_i (MΩ)	174.2 ± 5.8	302.3 ± 12.5	134.4 ± 15.9	97.2 ± 3.4	179.1 ± 10.6
	1 ≫ 4; 2 ≫ 1,3,4; 5 ≪ 2; 5 ≫ 4				
Threshold current (pA)	138.0 ± 7.6	119.0 ± 6.3	190.0 ± 7.6	182.6 ± 10.0	103.1 ± 11.6
	1 ≪ 4; 2 < 3; 2 ≪ 4; 5 < 3; 5 ≪ 4				
Interspike interval ratio (II_R)	1.70 ± 0.06	2.10 ± 0.10	4.46 ± 0.37	1.31 ± 0.44	1.18 ± 0.06
	1 ≪ 3; 1 ≫ 4; 2 ≫ 1,4; 2 ≪ 3; 3 ≫ 4; 5 ≪ 1,2,3				
Frequency (Hz)	38.8 ± 1.7	54.7 ± 2.2	43.5 ± 3.2	26.6 ± 0.9	118.8 ± 9.4
	1 ≫ 4; 2 ≫ 1,4; 3 ≫ 4; 5 ≫ 1,2,3,				
Number of spike/pulse	18.1 ± 1	23 ± 1	17 ± 2	13 ± 1	53 ± 5
	1 ≫ 4; 2 > 1; 2 ≫ 4; 5 ≫ 1,2,3,4				

Values are means ± SE; n, number of cells; >, significantly greater with $p<0.05$; ≫, significantly greater with $p<0.01$. Statistically significant comparisons were determined using Tukey post hoc analysis after performing ANOVA. RMP, resting membrane potential; R_I, input resistance; NAvHF, non-adapting very high frequency; AHF, adapting high frequency; ALF, adapting low frequency; sALF, strongly adapting low frequency; wALF, weakly adapting low frequency.

7.3, for 48 h at 4°C. The brains were then flash frozen in −80 °C isopentane for 50 s and stored at −80 °C until sectioning. The tissue was cut coronally (60 μm sections) on a cryostat at −15 °C. The free-floating sections were placed in cryoprotectant-filled tissue culture dishes and were stored at −20 °C in glycerol/PBS solution until they were ready to be processed.

Immunohistochemistry

The sections were washed with 0.5% Triton-X in PSB two times for 5 min and blocked with 10% normal serum in PSB with 0.025% Triton-X and 1% BSA for 1 h. The primary antibodies were diluted in PBS with 1% BSA and then pipetted into the tissue culture dish wells; the sections were incubated overnight at 4 °C. Sections were then washed with 0.5% Triton-X in PSB two times for 10 min, followed by application of a secondary antibody solution (diluted in PBS with 1% BSA) and incubated for 1 h at room temperature under low-light conditions. Sections were then rinsed with PBS three times for 10 min. Sections were wet mounted onto Fisher SuperFrost slides, covered with glass coverslips in Prolong Gold Antifade mounting medium (Molecular Probes, Eugene, OR), allowed to cure overnight at room temperature, and sealed the next day with nail polish. Slides were stored at −20 °C and protected from light until they were ready to be imaged.

Antibodies

The list of the primary and secondary antibodies used for PV/Kv1.6 colocalization experiment is provided below: Primary antibody monoclonal antiparvalbumin (mouse), diluted 1:2500 was obtained from Swant, Switzerland, catalog code 235, lot 10-11(F); primary antibody polyclonal anti Kv1.6 (rabbit), diluted 1:10,000, Abcam, US,

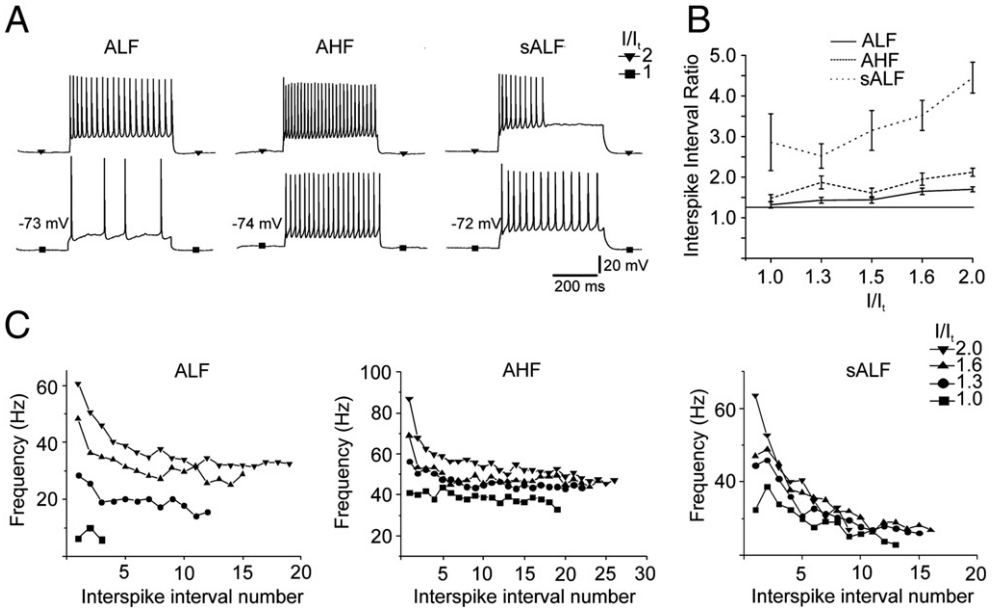

Fig. 2. Spiking properties of adapting firing cell types before kindling-induced epilepsy.

A. Traces show the response of adapting low frequency (ALF), adapting high frequency (AHF) and strongly adapting low frequency (sALF) cell types to injection of depolarizing current steps at threshold ($I/I_t = 1$) and twice the firing threshold ($I/I_t = 2$) levels.

B. Plot of the interspike interval ratio (II_R) against the level of injected current shows increased spike adaptation of sALF group and only a moderate adaptation for ALF and AHF groups ($II_R > 1.25$).

C. Plot of firing frequency against interspike interval number in a typical ALF, AHF and sALF cell. Note the high spike frequency adaptation at higher depolarization levels (twice the firing threshold) in the sALF cell type.

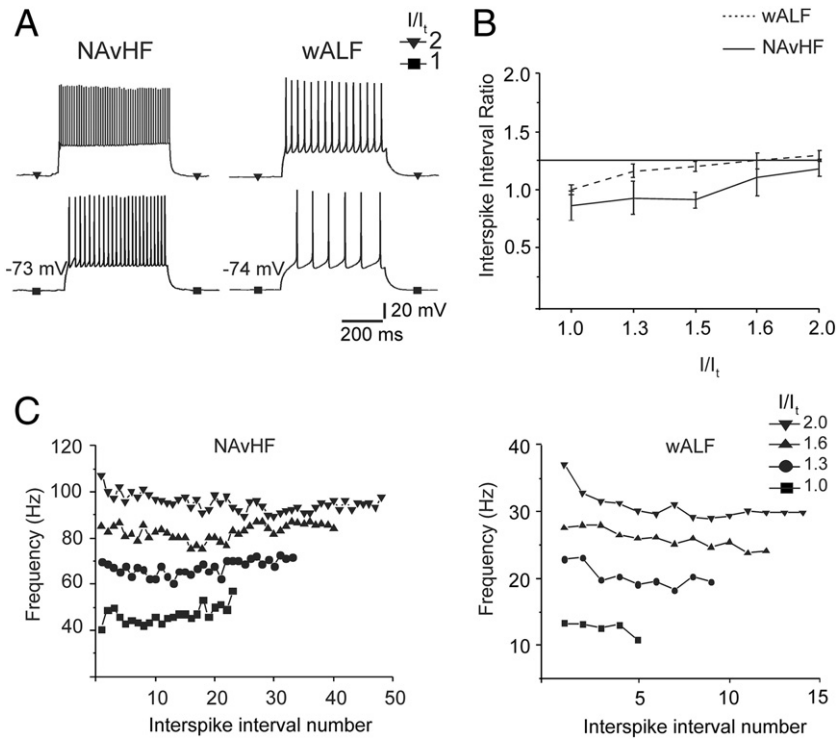

Fig. 3. Spiking properties of non-adapting and weakly adapting firing cell types before kindling-induced epilepsy.

A. Traces show the response of non-adapting very high frequency (NAvHF) and weakly adapting low frequency (wALF) cell types to injection of depolarizing current steps at threshold ($I/I_t = 1$) and twice the firing threshold ($I/I_t = 2$) levels.

B. The ratio between last and first interspike intervals (II_R) was plotted against level of injected current, showing the lack of significant firing adaptation in a typical NAvHF cell. Note the absence of spike frequency adaptation at lower depolarizing steps, while only a small firing adaptation was seen at higher depolarizing steps in a typical wALF cell.

C. Plot of firing frequency against interspike interval number in a typical NAvHF and wALF cell showing reduced firing adaptation levels ($II_R \leq 1.25$).

catalog # ab210089. Secondary antibodies: donkey anti mouse Alexa 488, diluted 1:1000, and goat anti rabbit Alexa 594 diluted 1:1000. The specificity of the secondary antibodies was verified in control sections in which the primary antibody was omitted. No staining was detected in omission control sections (data not shown).

For the CBP staining experiment we used the following antibodies: Primary antibody monoclonal antiparvalbumin (mouse), diluted 1:2500, Swant, Switzerland, catalog code 235, lot 10-11(F); primary polyclonal antibody anticalbindin (rabbit), 1:2500, Chemicon, Canada, catalog # AB1778; and primary polyclonal antibody anticalretinin (rabbit), 1:1000, Chemicon, Canada, catalog # AB5054. Secondary antibodies for PV staining: donkey anti mouse Alexa 488 (1:1000); for CB and CR staining: donkey anti rabbit Alexa 594 (1:1000).

Image acquisition and processing

In order to determine if the Kv1.6 protein had increased expression on parvalbumin (multipolar) interneurons, immunohistochemistry was performed on fixed brain slices (60 μm thick) with antibodies as described above. Confocal images were acquired on a Zeiss laser-scanning microscope (LSM 510 see Fig. 9B) using a water immersion 40× objective (N.A. = 1.2). Each image is a stack of 10–15 images 1 μm apart in the z-plane. This was performed for each wavelength channel. The stacks of confocal images were processed in IMARIS software (Bitplane, Zurich, Switzerland). The images were analyzed with the co-localization module using the criteria developed by us and described in Gavrilovici et al. (2010) and Hutcheon et al. (2004). The juxtaposed segmented pixels in the entire stack were converted to co-localized voxels (3-D) which were represented by a separate channel pseudo colored white. The number of resulting white voxels was counted in identical fields from control (n = 3) and kindled (n = 3) rats. The difference between the number of voxels was assessed using a *t*-test.

Results

The purpose of this study was to investigate the electrophysiological properties of interneuronal populations across all piriform cortex (PC) layers after kindling-induced epilepsy. The only recordings used for these studies were those where the morphology of the cell could be reconstructed after recording was completed (see Materials and methods). A total of 205 control brain recordings and 108 kindled brain recordings were used in the analysis.

In control brains, we found that the resting membrane potential (RMP) of PC interneurons ranged from −60 mV to −82 mV and no group of interneurons (described in detail below) were different from one-another based on RMP. All recordings could be broadly classified into two types of firings patterns. Most interneurons (180 cells; ~88%) responded by firing throughout the current injection (both

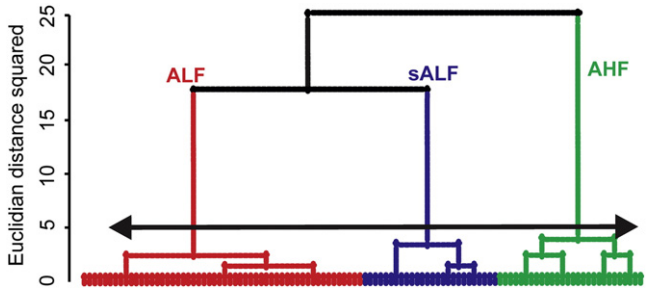

Fig. 4. Cluster analysis of electrophysiological properties of rat anterior piriform cortex interneuronal populations after kindling-induced epilepsy. The *x*-axis of dendrogram shows individual cells (n = 108) and the *y*-axis represents the linkage distance measured by Euclidean distance squared. Double arrow solid line represents the cut off showing three distinct clusters: adapting high frequency (AHF), adapting low frequency (ALF) and strongly adapting low frequency (sALF).

Table 2
Electrophysiological properties of the five types of interneuronal firing groups in the anterior piriform cortex in amygdala kindled rats.

	Cluster 1 ALF (n = 54)	Cluster 2 AHF (n = 27)	Cluster 3 sALF (n = 27)
RMP (mV)	−76.8 ± 0.7	−76.7 ± 1.1	−76.8 ± 1.1
R_i (MΩ)	152.1 ± 7.1 2 ≫ 1,3	301.2 ± 28.1	153.9 ± 9.3
Threshold current (pA)	153.7 ± 10.4 1,2 ≪ 3	131.4 ± 13.6	170.3 ± 13.1
Interspike Interval ratio (II_R)	1.66 ± 0.05 1,2 ≪ 3	1.86 ± 0.07	3.47 ± 0.13
Frequency (Hz)	29.1 ± 1.3 1 < 3; 2 ≫ 1,3	70.5 ± 3.9	37.0 ± 2.2
Number of spike/pulse	13 ± 1 2 ≫ 1; 2 > 3	22 ± 1	15 ± 1

Values are means ± SE; n, number of cells; >, significantly greater with $p<0.01$; ≫ significantly greater with $p<0.001$. Statistically significant comparisons were determined using Tukey post hoc analysis after performing ANOVA. RMP, resting membrane potential; R_i, input resistance; AHF, adapting high frequency; ALF, adapting low frequency; sALF, strongly adapting low frequency.

adapting and non-adapting firing patterns were observed in this group). The majority of the continuously firing interneurons (122 of 180 cells; ~68%) adapted to the stimulus. The occurrence of adaptation was defined by determining whether the last interspike firing interval was 25% longer than the first interval ($II_R > 1.25$). The remaining continuously firing interneurons (58 of 180 cells; ~32%), showed little or no firing adaptation ($II_R < 1.25$). We also found that adapting firing cells fired at both high (>50 Hz) and low (<50 Hz) frequencies. The rest (25 cells; ~12%) initially adapted but then eventually accommodated to the stimulus (i.e. they stopped firing before the end of the depolarizing step). Although this broad classification can provide some interesting functional aspects of PC interneurons, a more exact (unbiased) functional grouping was done by cluster analysis. Using these electrophysiological characteristics and others that we measured (see Materials and methods), we show that cluster analysis classified five distinct groups of interneurons (Fig. 1, Table 1). We have named these five groups: adapting low frequency (ALF), adapting high frequency (AHF), strongly adapting low frequency (sALF), non-adapting very high frequency (NAvHF) and weakly adapting low frequency (wALF). An examination of the differences in the attributes of these groups shows that they primarily segregated based on firing frequency (FF) and II_R although other attributes were statistically different between some groups (see Table 1).

In Fig. 2, we show three spiking patterns where adaptation and adaptation/accommodation were evident. The resting membrane potential for these cells was not different. Their phenotypes were primarily clustered based on their average FF, II_R and threshold current for their excitation. The most common firing pattern found was the ALF phenotype which at the highest stimulation intensity had an initial FF of about 58 ± 3 Hz. This rate declined to about 20 Hz ($II_R = 1.7$, Fig. 2A left panels and Table 1). Over the duration of the pulse these cells had an average FF of about 39 Hz. They accounted for about 35% (71 of 205) of all recordings. The second class of cells was the AHF type which initially fired action potentials at a rate of 91 ± 5 Hz but then adapted so that by the end of the current pulse the FF plateaued to about half this rate ($II_R = 2.1$). The average FF of these cells over the course of a pulse was 55 Hz (see Fig. 2 middle panels and Table 1). This phenotype accounted for about 20% of all recordings (42 of 205 cells). The third type of adapting firing pattern was the strongly adapting low frequency type (sALF: Fig. 2A). Although they initially fired at a high rate (93 ± 10 Hz) they strongly adapted to the stimulus so that their average firing frequency declined to around 15–20 Hz ($II_R = 4.4$) by the end of the current stimulus. The average FF was 43.5 ± 3.2 Hz over the course of the pulse. As well, these cells often accommodated to the stimulus at high current injection intensities but could sustain firing throughout the pulse at lower intensities. This phenotype was relatively rare in control slices accounting for only 5% of all recordings. The relationships between II_R and current intensities are shown in Fig. 2B for each of these cell

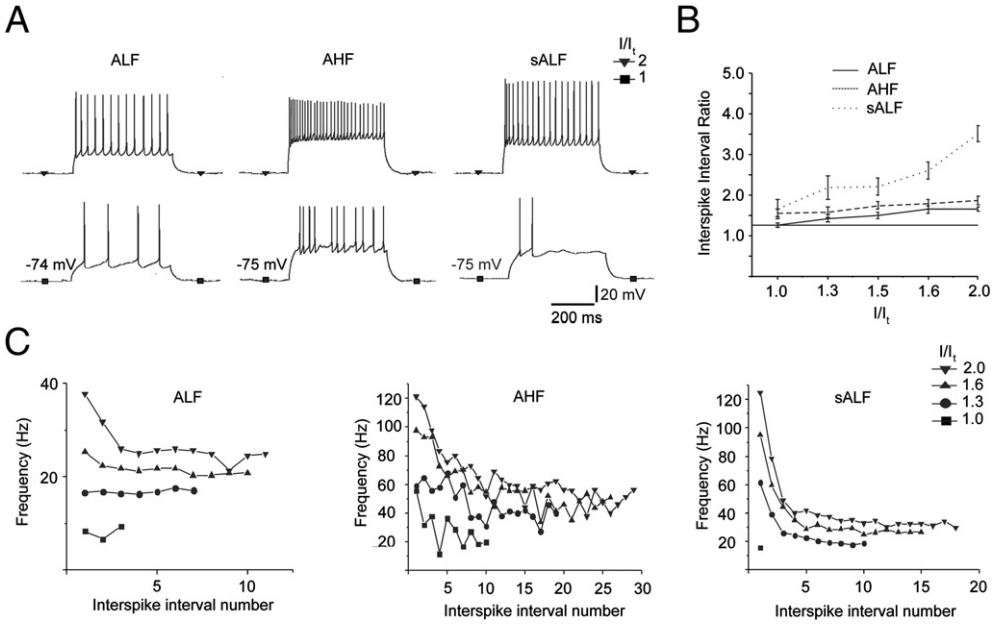

Fig. 5. Spiking properties of adapting firing cell types after kindling-induced epilepsy.

A. Traces show the response of adapting low frequency (ALF), adapting high frequency (AHF) and strongly adapting low frequency (sALF) cell types to injection of depolarizing current steps at threshold ($I/I_t = 1$) and twice the firing threshold ($I/I_t = 2$) levels.

B. The ratio between last and first interspike intervals (II_R) was plotted against level of injected current, showing moderate level of firing adaptation across ALF and AHF group and increased firing adaptation across sALF group ($II_R > 1.25$).

C. Plot of firing frequency against interspike interval number in a typical ALF, AHF and sALF cell. Note the high spike frequency adaptation at higher depolarization levels (twice the firing threshold) in the sALF cell type.

types. For ALF and AHF types the II_R was roughly the same over the current intensities used. Only the sALF showed a trend to more adaptation as current intensity was increased. The AHF had the highest threshold for firing in comparison with the ALF and sALF interneurons whose thresholds were not statistically different. In Fig. 2C we show the firing patterns and stimulation intensity for three representative cells within this adapting class of interneuronal firing pattern.

The next broad class of firing patterns found were those that adapted very little or not at all during the stimulus pulse. Thus their FF was relatively constant over the current pulse. However, the frequency at which they fired on average increased as current intensity was increased. The first subdivision of this class of interneurons was the non-adapting very high frequency type (NAvHF, II_R of 1.18 ± 0.06; Table 1; Fig. 3A, left panels). These cells had the highest initial firing frequency among all PC interneuronal groups and were able to sustain this activity throughout the pulse. They generated action potentials in the range of 100–150 Hz at maximum current intensities (average 118.8 ± 9.4 Hz; Table 1; Figs. 3A and B). These cells were also more excitable, having a significantly lower firing threshold than all other cell types (see Table 1 in Fig. 1). This phenotype was found in 16 of 205 recordings. The second type of firing pattern identified within the non-adapting class were those that fired at low frequencies ($FF = 26.6 \pm 0.9$ Hz, Fig. 3A, right panels). The wALF group represented about 32% of all cells (66 of 205 recordings) and was therefore the second largest group of interneurons. The wALF cells had the lowest input resistance of all cells and a much higher threshold current than NAvHF group. The average resting membrane potential of these two cell phenotypes was, however, not statistically different (see Table 1).

Next we determined if the firing patterns we had found on the control rats were changed after the induction of stage 5 seizures by kindling the basal lateral amygdala. All recordings were performed on rats that had stage 5 seizures over a period of 6 consecutive days. Rats were allowed to recover from their last seizure for a minimum of two weeks before being sacrificed for patch clamp recording. Our initial qualitative analysis of these data showed that both the NAvHF and wALF phenotypes were not found in this cohort of recordings. Cluster analysis of the same parameters measured in control recordings confirmed this and showed that only three types of behaviors could be classified: ALF, AHF and sALF phenotypes. In Fig. 4 and Table 2, we show the cluster dendrogram and the traits of the three clusters that were identified. The attributes of these three types were not different from the corresponding groups identified in control recordings (see Fig. 5 and compare Table 1 with Table 2). As seen in control, the ALF phenotype initially fired at a rate of 51.3 ± 2.4 Hz ($p = 0.81$) and declined to about 30 Hz ($II_R = 1.66$). The AHF fired at frequencies of 103.7 ± 6.5 Hz ($p = 0.48$) but was only about 50 Hz at the end of the pulse ($II_R = 1.87$). Only the sALF phenotype was slightly different. Although it initially fired like controls (90.8 Hz, $p = 1.0$) it adapted less than in control tissue ($II_R = 3.4 \pm 0.1$ in kindled vs. $II_R = 4.4 \pm 0.3$ in control group; $p < 0.01$). We did not find either the NAvHF or the wALF phenotypes in the kindled

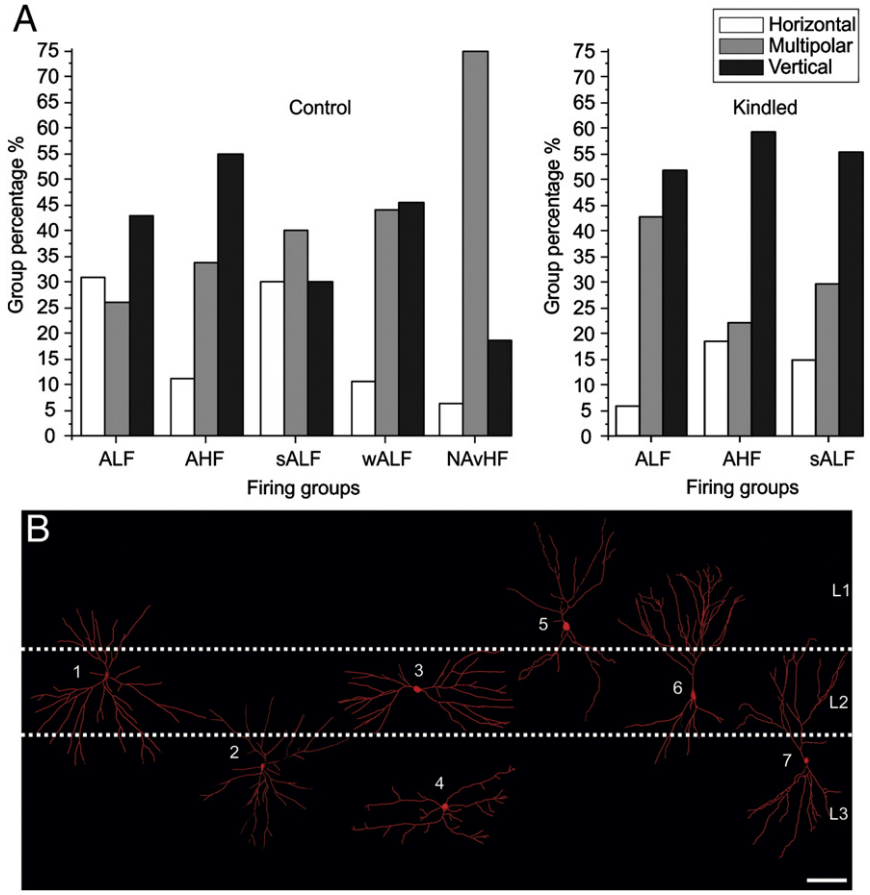

Fig. 6. Correlation between the firing pattern types and interneuronal morphology in the piriform cortex before and after kindling-induced epilepsy.

A. Vertical bars represent the percent of horizontal, multipolar and vertical cells in each firing group: ALF, adapting low frequency; AHF, adapting high frequency; sALF, strongly adapting low frequency; NAvHF, non-adapting very high frequency; wALF, weakly adapting low frequency.

B. Localization and morphologies of interneurons within the anterior piriform cortex. Examples of interneurons with multipolar (cell 1 in layer 2 and cell 2 in layer 3), horizontal (cell 3 and cell 4 in layers 2 and 3) and vertical morphologies (cell 5, cell 6 and cell 7 in layers 1, 2 and 3 of the piriform cortex). L1, layer 1; L2, layer 2; L3, layer 3; Scale bar = 40 μm.

brains. To determine if these observations could have occurred by chance a chi-square analysis was done. This analysis gave a χ^2 value of 7.1 ($p<0.01$) between control and kindled for the NAvHF phenotype and a χ^2 value of 41.0 ($p<0.0001$) for the wALF group. This analysis indicates that the chance that these two phenotypes were not observed in the kindled brain is not due to a sample size. We also found that, similar to control rats, the resting membrane potential (RMP) of PC interneurons after kindling ranged from −61 mV to −86 mV and no group of interneurons was different from another based on RMP, input resistance, threshold, or FF. Importantly, the two firing patterns that were not seen in kindled brain slices accounted for 40% of all the recordings. This "shift" in function resulted in a substantial increase in the proportion of neurons having the sALF phenotype. This phenotype represented only 5% of all recordings in control brain slices but represented 25% of all recordings after kindling ($\chi^2=25.6$, $p<0.001$). There was also a significant change in the proportion of cells that were ALF, from 35% in control to 50% after kindling ($\chi^2=6.3$, $p<0.025$). There was no change in the proportion of cells that had the AHF phenotype ($\chi^2=0.6$, $p>0.05$). Overall, interneurons in the kindled brain are unable to sustain very high frequency firing and lose the ability to have sustained firing due to a prolonged stimulus. By contrast, we found no change in the attributes (amplitude or duration) of individual spikes between control and kindled brain (ps = 0.78–1.0 for group comparisons). These data show that after kindling there is a significant change in the firing patterns of 40% of all interneurons.

Next, we determined if the firings patterns were unique to the morphology and/or location of the interneurons in the control and kindled groups. In our previous work we had shown that interneurons of the PC can be categorized into three main morphologies: multipolar, horizontal and vertical (Gavrilovici et al., 2010). In Fig. 6B we show examples of our reconstructions done after each recording and their location within the three layers of the PC. Vertical cells are located in all three layers and have been previously identified as uniquely calretinin (CR) positive (see Fig. 6B cells 5, 6 and 7 and Gavrilovici et al., 2010). The horizontal cells are calbindin (CB) positive (see Fig. 6B cells 3 and 4) and the multipolar cells are parvalbumin (PV) positive but may also co-express CB, and were found in layers 2 and 3 but not layer 1 (Fig. 6A cells 1 and 2). In control slices we found that generally the spiking patterns were not consistently predictive of a specific interneuronal morphology/location. The exception to this observation was that most cells (12/16) displaying the NAvHF phenotype were multipolar. The wALF phenotype was rarely seen in the horizontal cells (7/66), but was observed in equal numbers of multipolar and vertical cells (30 and 29 of 66 recordings, respectively). The other three phenotypes (all having an adapting firing pattern) did not show a strong "preference" towards any of the detected morphological types (Fig. 6A). After kindling, a change in these proportions was found. The ALF pattern was recorded in 60% of the kindled multipolar interneurons compared to 28% in control ($\chi^2=10.6$, $p<0.005$). No change in the proportion of horizontal or vertical cells was found. These results indicate that many multipolar cells are changing their firing properties from either NAvHF or wALF to ALF. Similarly after kindling the sALF phenotype was found in higher proportions in all morphologies. In control brains, the sALF phenotype was found in only 5%, 4% and 6% of multipolar, vertical and horizontal cells but after kindling 21%, 34% and 26% were found to have this firing pattern respectively ($\chi^2=6.0$, 11.3 and 4.3, $ps<0.05$).

Finally, to rule out the idea that the loss of these firing patterns was due to cell death we counted the number of CR, CB and PV immunopositive cells before and after kindling. The number and relative proportion of these cell types remained consistent. From our morphological reconstructions (after recordings) the relative frequency of horizontal, multipolar and vertical cells in control rats was unchanged after kindling (16% were horizontal in control rats as compared to 11% horizontal cells after kindling, $\chi^2=0.842$, $p>0.05$; multipolar cells were 38% before and 36% after kindling, $\chi^2=0.498$, $p>0.05$ and vertical cells: 46% before and 54% after kindling, $\chi^2=2.07$, $p>0.05$). A count of CB, PV and CR positive cells in sections before and after kindling also confirmed that there was no change in the number and proportion of these cell types (χ^2 all less than 1.0, $p>0.05$). Overall, our observations indicate that the interneurons of the PC change their firing patterns and this is not due to the selective loss of one or more kinds of interneurons.

Next we wanted to determine by what mechanism these alterations in firing patterns may occur. It has been suggested that $GABA_A$ receptor activity can modulate the adaptation and firing properties of neurons (Prescott and Koninck, 2003). Since previous studies (Gavrilovici et al., 2006; Meguro et al., 2004) have shown that $GABA_A$ receptor expression and synaptic currents are increased on interneurons after kindling, we tested whether blocking this activity may alter the spiking patterns of these cells. However, we found no evidence of this as blocking either synaptic activity and/or extrasynaptic activity with GABAzine had no effect (see Fig. 7). Having ruled this possibility out, we turned our attention to potassium currents as they are well known modulators of cellular excitability. As shown in Fig. 8, after blockade of all other voltage dependent currents (Na^+ and Ca^{2+}), we found that in multipolar cells the outward whole cell potassium

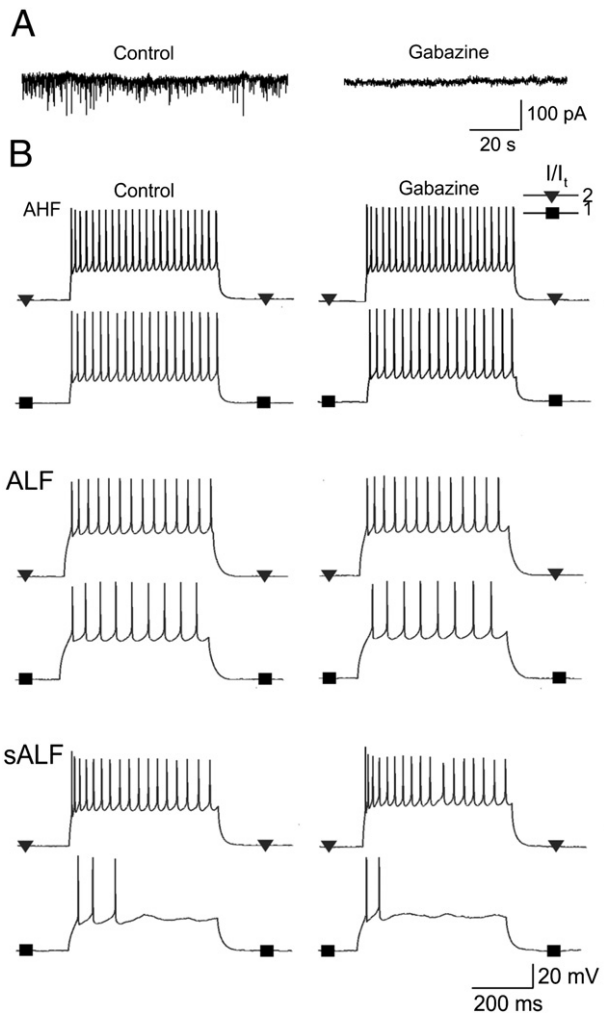

Fig. 7. Gabazine effect on firing patterns of piriform cortex interneurons. A. Gabazine (10 μM) blocked GABAergic currents on PC interneurons (n = 9). In B, we show that gabazine (10 μM) did not alter the firing pattern of interneurons (n = 25). Here we show one example for each firing cluster: AHF (top traces), ALF (middle) and sALF (bottom) interneuron response to injection of depolarizing current at threshold ($I/I_t=1$) and twice the firing threshold ($I/I_t=2$) levels. AHF, adapting high frequency; ALF, adapting low frequency; sALF, strongly adapting low frequency.

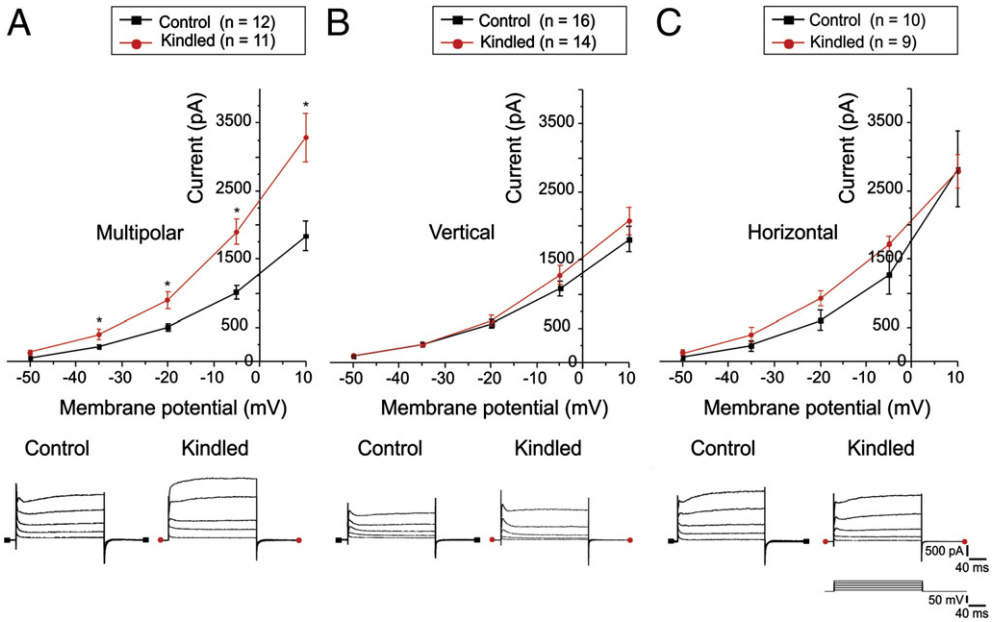

Fig. 8. The voltage-dependent potassium current in the piriform cortex interneurons before and after kindling-induced epilepsy. Potassium outward currents were evoked by depolarizing steps between −50 and +10 mV in multipolar (A), vertical (B) and horizontal (C) piriform cortex interneurons. The current–voltage (*I–V*) relationships showed an increased K^+ current after kindling in multipolar but no change was seen in vertical and horizontal cells. Outward currents were measured at the end of each depolarizing voltage pulse (bottom traces). Error bars represent the standard error of the mean. Statistically significant comparisons were determined using *t*-test, $^*p<0.05$.

currents were indeed substantially increased. In vertical cells we found no difference and in horizontal cells there was a small increase but this did not reach statistical significance. Thus at least in multipolar cells there is an increase in long lasting potassium current.

Next to identify the potassium channel(s) whose expression was up-regulated we assayed for changes in the expression of mRNAs coding all known voltage dependent channel genes in rats (see Materials and methods) using a commercially available QPCR array. We used four arrays, 2 for control and 2 for kindled. In each array we seeded the wells with cDNA made from total cellular RNA isolated from PC. We pooled the cDNA from either 5 control or 5 kindled rats. The expression was normalized to 3 different reference genes on the aarrays and the differences in expression between arrays were calculated as a $\Delta\Delta C_t$. We found mRNAs that code for 4 potassium channels were up-regulated in the kindled brains $\Delta\Delta C_t > 1.0$. These were Kv1.2, 1.6, 2.1 and 9.3 subtypes. To statistically validate these data we then analyzed the expression of these 4 mRNAs from 11 control rats and 9 kindled rats individually. This analysis showed that only the Kv1.6 mRNA was increased in the expression (Fig. 9A). In order to see if the Kv1.6 protein was increased on PV positive (multipolar) cells we did immunohistochemistry and examined the co-localization of the PV with Kv1.6 protein in perfusion fixed brain slices. In the control slices little if any Kv1.6 expression was observed (Fig. 9B) but this was not the case after kindling. There was an increase of Kv1.6 protein on the PV positive cells and puncta which have previously been shown to be PV nerve terminals (see Gavrilovici et al., 2010). A quantitative analysis of the PV/Kv1.6 signal (see Materials and methods) showed about 400% increase in the number of co-localized voxels after kindling ($p = 0.0013$, Fig. 9B).

These data show that multipolar PV positive interneurons have an increase in Kv1.6 potassium channel protein thus accounting for the increase in potassium currents in these cells.

Discussion

Our study identifies multiple subpopulations of interneurons with different firing patterns and membrane properties in all three layers of rat aPC. The five interneuron phenotype clusters were named according to the previously described terminology developed by Ascoli et al. (2008) and Kroner et al. (2007). Although this classification system may not fully describe all the fine details of the firing patterns, it does describe their predominate behaviors. This main finding shows that there was a shift to adapting firing modes at the expense of non-adapting very high frequency (NAvHF) and weakly adapting low frequency (wALF) firing. Thus there is a loss of complexity in the interneuron firing patterns. These alterations in firing patterns are not linked to a change of passive membrane properties in line with other studies in the hippocampus after kindling (Mody and Staley, 1994). The change in firing patterns was attributed to an increase in the expression of the voltage dependent potassium current, Kv1.6. Our immunohistochemical analysis of CBP containing interneurons also revealed a similar distribution of interneurons before and after kindling in agreement with the findings of another study (Lehmann et al., 1996). As the hallmark of interneuron function is their diverse firing patterns our observations suggest that epilepsy may be associated with a loss of this functional complexity; a change that predicts a significant impact on the neural circuit in which they function.

We also found that the passive membrane properties of interneuronal populations were unchanged after kindling, and $GABA_A$ blockade did not change the firing patterns of interneurons. Only an increase in potassium channel activity could be correlated to the activity seen after kindling. The Kv1.6 is part of the delayed rectifier class (Kv1 class, shaker-related subfamily), along with Kv1.1–1.3 and Kv1.5 that generate sustained outward Kv currents (Gutman et al., 2005; Hille, 2001) as opposed to Kv1.4 which mediates transient (A-type) outward K^+ current (Vacher et al., 2008). The attributes of the Kv1.6 currents fit well with those recorded here. The lack of a specific Kv1.6 channel blocker prevents us from conclusively showing that we could revert to control phenotype after kindling and so while our data strongly indicate that this potassium channel variant is responsible for these wide ranging changes it cannot be pharmacologically confirmed at this time.

We show that in general PC interneurons after kindling are less excitable and therefore would be less able to provide the same level of inhibitory “strength”. In another study, we have also shown after

kindling miniature inhibitory post synaptic currents (mIPSCs) are larger and longer lasting on interneurons, effectively doubling the current density of a single mIPSC (Gavrilovici et al., 2006). We have also provided evidence that PV immunopositive puncta are likely GABA release sites (Gavrilovici et al., 2010) and here we show that these puncta have increased the expression of the Kv1.6 protein (see Fig. 9B). Thus nerve terminals may be less excitable and transmitter release may be reduced. Overall, the combination of these outcomes predict profound effects on the net inhibition that can be provided to the pyramidal cell layer since it is the multipolar PV/CB positive neurons that provide the bulk of somatic inhibition to the pyramidal cell layer. Thus our observations suggest that after kindling interneurons generate fewer action potentials, may have reduced probability of GABA release, and are more inhibited by other interneurons. Overall these changes likely contribute to the seizure activity.

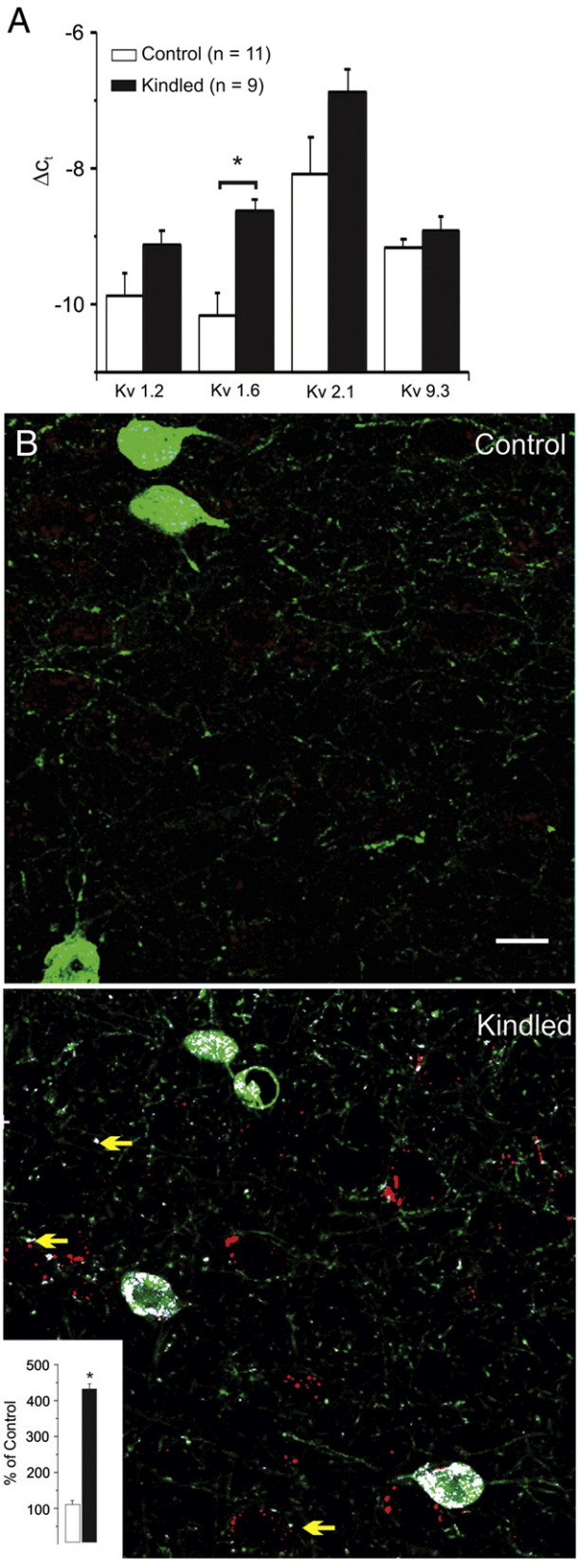

The changes found here may also predict very large perturbations in the rhythmicity of PC networks. In PC, oscillatory activities are considered part of olfactory processing and memory coding (Neville and Haberly, 2004) however little is known about the role that different classes of interneurons found here play in PC oscillatory behavior. The importance of interneurons function in this regard has been established in hippocampus and neocortex. Functionally unique interneurons target specific pyramidal cell compartments (somatic or dendritic) that differentially participate in network oscillations in hippocampal area (Chapman and Lacaille, 1999; Maccaferri and McBain, 1996; Pike et al., 2000) and in entorhinal cortex (Middleton et al., 2008). Importantly it has been shown that the firing patterns of interneurons are often well matched to the oscillations in which they participate. For example, Lacunosum-moleculare interneurons that would be classified as ALF here have been suggested to be important in generating theta rhythms in the hippocampus (Chapman and Lacaille, 1999; Maccaferri et al., 2000). Similarly, fast spiking basket cells (similar to AHF and perhaps NAvHF) are important for the generation of faster gamma rhythms (Fuchs et al., 2007; Sohal et al., 2009). Based on these studies and our own recent immunocytochemical data showing that L2 and L3 multipolar cells provide the bulk of pyramidal cell (somatic) inhibition (Gavrilovici et al., 2010), it seems that they are obvious candidates for being involved in both theta and gamma rhythms, depending on their firing pattern. By analogy, the loss of the NAvHF phenotype suggests that high frequency network oscillations may be more difficult to create or sustain after kindling. Furthermore, the substantial increase in the number of cells that fire at low or more readily adapting rates suggests a propensity to have relatively low frequency network oscillations. As slow wave oscillations are a hallmark of epileptic activity (McIntyre et al., 2002b) this change in interneuron network control would therefore seem to favor seizure generation.

Our morphological reconstructions classified three main groups based on the dendritic arborization patterns we have previously shown (Gavrilovici et al., 2010). As mentioned in the Material and methods our analysis does not include neurogliaform interneurons, as sufficient recordings were not obtained to provide a valid comparison. Indeed the spiking patterns reported for these cells in mouse aPC by Suzuki and Bekkers (2010) were never detected in over 600 recordings that we performed in rat aPC. In Suzuki and Bekkers's (2010)

Fig. 9. QPCR and immunohistochemistry analysis of voltage gated potassium channels before and after kindling.

A. Delta C_t analysis of four voltage-gated potassium channels' mRNA expression in rat anterior piriform cortex before and after kindling-induced epilepsy. Comparison between control and kindled groups indicates increased expression of Kv1.6 after kindling. Test genes are listed on the x axis while ΔC_t values are shown on the y axis. Significant differences ($^*p<0.05$) are listed with an asterisk.

B. Parvalbumin/Kv1.6 colocalization in rat piriform cortex before and after kindling-induced epilepsy. Green channel shows parvalbumin immunoreactivity (PV-IR); red signal represents Kv1.6-IR; white pixels indicate PV and Kv1.6 colocalized segments. Low level of PV/Kv1.6 colocalization is found in control tissue (top), while higher expression of PV/Kv1.6 is seen in PV interneurons after kindling (bottom). Yellow arrows indicate PV/Kv1.6 puncta and are believed to be inhibitory nerve terminals.

characterization of the mouse PC they found 6 spiking patterns that included 2 firing patterns for neurogliaform cells. However, here we have found 5 distinct firing patterns that do not include this phenotype. According to our nomenclature Suzuki and Bekkers (2010) found NAvHF, sALF, ALF and wALF in the vertical, multipolar and horizontal (CBP positive) interneurons. They also observed that while some morphological subtypes tended to fire with a dominant pattern, like found here, this was not always the case. For example, multipolar cells fired at both high and relatively low frequencies. These observations are similar to other reports. A lack of correspondence between morpho-electrophysiological characteristics was described in neocortical and hippocampus interneurons where cells with the same morphological type had different membrane properties and firing patterns (Mott et al., 1997; Parra et al., 1998). The firing heterogeneity is thought to result from different distributions/expressions of various ionic channels on cell's membrane and/or morphological features (Llinas, 1988; Mainen and Sejnowski, 1996). In any case while the mouse PC has many similarities to rat there appears to be distinct differences with the rat having at least one more mode of firing (AHF). Nevertheless morphologically distinct interneurons have multiple modes of firing reflecting perhaps a division in the control of PC neural oscillations.

Alterations in the expression of genes encoding many voltage gated potassium channels have been reported in human epilepsies and animal model of epilepsies (see review Lukasiuk et al., 2007). In amygdala kindling, increased expression of Kv4.2, Kv4.3 and Kv7.2 immunoreactivity (Chang et al., 2006; Penschuck et al., 2005) was reported in the amygdala region and (Corcoran et al., 2011) showed that kindling the amygdala induced an increased expression of KCNF1, Kv7.1 in amygdala. However, changing the site of kindling to the hippocampus increased the expression of KCNF1 in the hippocampus and Kv3.4 in the amygdala but decreased KCNA3, Kv7.1 and KCNF1 expression in the amygdala. In the pilocarpine-induced animal model of epilepsy, Kv1.4 immunoreactivity was increased in the dentate molecular layer while Kv4.2 expression was decreased in the stratum radiatum of CA1 post SE (Monaghan et al., 2008). Similarly, pilocarpine decreased expression of Kv4.2 in CA1 region leading to a Kv4.2-dependent enhanced excitability was also confirmed by others (Bernard et al., 2004; Su et al., 2008). These studies showed a plethora of voltage gated K^+ channel alterations following chemical or electrical induced epilepsy. This suggests that the alterations in channel expression are dependent on the attributes of the afterdischarges/seizures that are generated from these various models of epilepsy. If so, this may explain to some extent the varied nature of epilepsies which are highly heterogeneous. However, the functional impact of these changes has not been reported in any of these studies.

The present study shows a wide spread and important loss in the diversity of interneuron function in an experimental model of temporal lobe epilepsy. How exactly these changes may produce seizures is not clear at this time but as interneurons are central to the control of neural network oscillations these changes likely disturb the timing of this circuit. As well the molecular pathways that kindling activates to increase the expression of this and perhaps other potassium channel genes would be important to understand as well as how wide spread this plasticity may be. This knowledge would be important for better understanding of how seizures may become progressively worse and provide novel targets for treatment that prevent the exacerbation of the seizures particularly among those with drug resistant epilepsy.

Acknowledgments

We would like to thank Professor John F MacDonald for his critical reading of the manuscript. This work was supported by the Canadian Institutes of Health Research Operating grant to MOP (grant number 1758356). CG was supported by an Ontario Graduate Student Fellowship.

References

Ascoli, G.A., Alonso-Nanclares, L., Anderson, S.A., Barrionuevo, G., Benavides-Piccione, R., Burkhalter, A., Buzsáki, G., Cauli, B., Defelipe, J., Fairén, A., Feldmeyer, D., Fishell, G., Fregnac, Y., Freund, T.F., Gardner, D., Gardner, E.P., Goldberg, J.H., Helmstaedter, M., Hestrin, S., Karube, F., Kisvárday, Z.F., Lambolez, B., Lewis, D.A., Marin, O., Markram, H., Muñoz, A., Packer, A., Petersen, C.C., Rockland, K.S., Rossier, J., Rudy, B., Somogyi, P., Staiger, J.F., Tamas, G., Thomson, A.M., Toledo-Rodriguez, M., Wang, Y., West, D.C., Yuste, R., 2008. Petilla terminology: nomenclature of features of GABAergic interneurons of the cerebral cortex. Nat. Rev. Neurosci. 9 (7), 557–568.

Bernard, C., Anderson, A., Becker, A., Poolos, N.P., Beck, H., Johnston, D., 2004. Acquired dendritic channelopathy in temporal lobe epilepsy. Science 305 (5683), 532–535.

Cauli, B., Porter, J.T., Tsuzuki, K., Lambolez, B., Rossier, J., Quenet, B., Audinat, E., 2000. Classification of fusiform neocortical interneurons based on unsupervised clustering. Proc. Natl. Acad. Sci. U. S. A. 97 (11), 6144–6149.

Chang, H.H., Su, T., Sun, W.W., Zhao, Q.H., Qin, B., Liao, W.P., 2006. Changes of potassium channels Kv4.2, Kv4.3 and Kv channel interacting protein 1 in amygdala kindling epilepsy: experiment with rats. Zhonghua Yi Xue Za Zhi 86 (47), 3315–3318.

Chapman, C.A., Lacaille, J.C., 1999. Intrinsic theta-frequency membrane potential oscillations in hippocampal CA1 interneurons of stratum lacunosum-moleculare. J. Neurophysiol. 81 (3), 1296–1307.

Corcoran, M.E., Kroes, R.A., Burgdorf, J.S., Moskal, J.R., 2011. Regional changes in gene expression after limbic kindling. Cell. Mol. Neurobiol. 31 (6), 819–834.

Dietrich, D., Podlogar, M., Ortmanns, G., Clusmann, H., Kral, T., 2005. Calbindin-D28k content and firing pattern of hippocampal granule cells in amygdala-kindled rats: a perforated patch-clamp study. Brain Res. 1032 (1–2), 123–130.

Ekstrand, J.J., Domroese, M.E., Feig, S.L., Illig, K.R., Haberly, L.B., 2001. Immunocytochemical analysis of basket cells in rat piriform cortex. J. Comp. Neurol. 434 (3), 308–328.

Fuchs, E.C., Zivkovic, A.R., Cunningham, M.O., Middleton, S., Lebeau, F.E., Bannerman, D.M., Rozov, A., Whittington, M.A., Traub, R.D., Rawlins, J.N., Monyer, H., 2007. Recruitment of parvalbumin-positive interneurons determines hippocampal function andassociated behavior. Neuron 53 (4), 591–604.

Gavrilovici, C., D'Alfonso, S., Dann, M., Poulter, M.O., 2006. Kindling-induced alterations in $GABA_A$ receptor mediated inhibition and neurosteroid activity in the piriform cortex of rat. Eur. J. Neurosci. 24, 1373–1384.

Gavrilovici, C., D'Alfonso, S., Poulter, M.O., 2010. Diverse interneuron populations have highly specific interconnectivity in the rat piriform cortex. J. Comp. Neurol. 518 (9), 1570–1588.

Gutman, G.A., Chandy, K.G., Grissmer, S., Lazdunski, M., McKinnon, D., Pardo, L.A., Robertson, G.A., Rudy, B., Sanguinetti, M.C., Stühmer, W., Wang, X., 2005. International Union of Pharmacology. LIII. Nomenclature and molecular relationships of voltage-gated potassium channels. Pharmacol. Rev. 57 (4), 473–508.

Haberly, L.B., 1983. Structure of the piriform cortex of the opossum. I. Description of neuron types with Golgi methods. J. Comp. Neurol. 213 (2), 163–187.

Haberly, L.B., 2001. Parallel-distributed processing in olfactory cortex: new insights from morphological and physiological analysis of neuronal circuitry. Chem. Senses 26 (5), 551–576.

Haberly, L.B., Price, J.L., 1978. Association and commissural fiber systems of the olfactory cortex of the rat. J. Comp. Neurol. 178 (4), 711–740.

Haberly, L.B., Hansen, D.J., Feig, S.L., Presto, S., 1987. Distribution and ultrastructure of neurons in opossum piriform cortex displaying immunoreactivity to GABA and GAD and high-affinity tritiated GABA uptake. J. Comp. Neurol. 266 (2), 269–290.

Hille, B., 2001. Potassium channels and chloride channels. Ion Channels of Excitable Membranes. Sinauer Associates, Sunderland, Mass.

Hutcheon, B., Fritschy, J.M., Poulter, M.O., 2004. Organization of GABA receptor alpha-subunit clustering in the developing rat neocortex and hippocampus. Eur. J. Neurosci. 19 (9), 2475–2487.

Kanter, E.D., Haberly, L.B., 1993. Associative long-term potentiation in piriform cortex slices requires GABAA blockade. J. Neurosci. 13 (6), 2477–2482.

Kelly, M.E., Staines, W.A., McIntyre, D.C., 2002. Secondary generalization of hippocampal kindled seizures in rats: examining the role of the piriform cortex. Brain Res. 957 (1), 152–161.

Klausberger, T., Somogyi, P., 2008. Neuronal diversity and temporal dynamics: the unity of hippocampal circuit operations. Science 321 (5885), 53–57.

Kroner, S., Krimer, L.S., Lewis, D.A., Barrionuevo, G., 2007. Dopamine increases inhibition in the monkey dorsolateral prefrontal cortex through cell type-specific modulation of interneurons. Cereb. Cortex 17 (5), 1020–1032.

Lehmann, H., Ebert, U., Loscher, W., 1996. Immunocytochemical localization of GABA immunoreactivity in dentate granule cells of normal and kindled rats. Neurosci. Lett. 212 (1), 41–44.

Llinas, R.R., 1988. The intrinsic electrophysiological properties of mammalian neurons: insights into central nervous system function. Science 242 (4886), 1654–1664.

Loscher, W., Ebert, U., 1996. The role of the piriform cortex in kindling. Prog. Neurobiol. 50 (5–6), 427–481.

Loscher, W., Lehmann, H., Ebert, U., 1998. Differences in the distribution of GABA- and GAD-immunoreactive neurons in the anterior and posterior piriform cortex of rats. Brain Res. 800 (1), 21–31.

Lukasiuk, K., Dingledine, R., Lowenstein, D., Pitkanen, A., 2007. Gene expression underlying changes in network excitability. In: Engel, J., Pedley, T. (Eds.), Epilepsy: A Comprehensive Textbook. Lippincott Williams and Wilkins, Philadelphia, pp. 307–322.

Luskin, M.B., Price, J.L., 1983. The topographic organization of associational fibers of the olfactory system in the rat, including centrifugal fibers to the olfactory bulb. J. Comp. Neurol. 216 (3), 264–291.

Maccaferri, G., McBain, C.J., 1996. The hyperpolarization-activated current (Ih) and its contribution to pacemaker activity in rat CA1 hippocampal stratum oriens–alveus interneurones. J. Physiol. 497 (1), 119–130.
Maccaferri, G., Roberts, J.D., Szucs, P., Cottingham, C.A., Somogyi, P., 2000. Cell surface domain specific postsynaptic currents evoked by identified GABAergic neurones in rat hippocampus in vitro. J. Physiol. 524 (1), 91–116.
Mainen, Z.F., Sejnowski, T.J., 1996. Influence of dendritic structure on firing pattern in model neocortical neurons. Nature 382 (6589), 363–366.
McIntyre, D.C., Molino, A., 1972. Amygdala lesions and CER learning: long term effect of kindling. Physiol. Behav. 8 (6), 1055–1058.
McIntyre, D.C., Plant, J.R., 1993. Long-lasting changes in the origin of spontaneous discharges from amygdala-kindled rats: piriform vs. perirhinal cortex in vitro. Brain Res. 624 (1–2), 268–276.
McIntyre, D.C., Hutcheon, B., Schwabe, K., Poulter, M.O., 2002a. Divergent GABA(A) receptor-mediated synaptic transmission in genetically seizure-prone and seizure-resistant rats. J. Neurosci. 22 (22), 9922–9931.
McIntyre, D.C., Poulter, M.O., Gilby, K., 2002b. Kindling: some old and some new. Epilepsy Res. 50 (1–2), 79–92.
Meguro, R., Lu, J., Gavrilovici, C., Poulter, M.O., 2004. Static, transient and permanent organisation of $GABA_A$ receptor expression in calbindin positive interneurons in response to amygdala kindled seizures. J. Neurochem. 91 (1), 144–154.
Middleton, S., Jalics, J., Kispersky, T., LeBeau, F.E., Roopun, A.K., Kopell, N.J., Whittington, M.A., Cunningham, M.O., 2008. NMDA receptor-dependent switching between different gamma rhythm-generating microcircuits in entorhinal cortex. Proc. Natl. Acad. Sci. U. S. A. 105 (47), 18572–18577.
Mody, I., Staley, K.J., 1994. Cell properties in the epileptic hippocampus. Hippocampus 4 (3), 275–280.
Monaghan, M.M., Menegola, M., Vacher, H., Rhodes, K.J., Trimmer, J.S., 2008. Altered expression and localization of hippocampal A-type potassium channel subunits in the pilocarpine-induced model of temporal lobe epilepsy. Neuroscience 156 (3), 550–562.
Mott, D.D., Turner, D.A., Okazaki, M.M., Lewis, D.V., 1997. Interneurons of the dentate-hilus border of the rat dentate gyrus: morphological and electrophysiological heterogeneity. J. Neurosci. 17 (11), 3990–4005.
Neville, K.R., Haberly, L.B., 2003. Beta and gamma oscillations in the olfactory system of the urethane-anesthetized rat. J. Neurophysiol. 90 (6), 3921–3930.
Neville, K.R., Haberly, L.B., 2004. Olfactory cortex. In: Shepherd, G.M. (Ed.), The Synaptic Organization of the Brain. Oxford University Press, New York, pp. 415–454.
Parra, P., Gulyas, A.I., Miles, R., 1998. How many subtypes of inhibitory cells in the hippocampus? Neuron 20 (5), 983–993.
Paxinos, G., Watson, P.L., 1986. The Rat Brain in Stereotaxic Coordinates, second ed. Academic Press, Sydney.
Penschuck, S., Bastlund, J.F., Jensen, H.S., Stensbol, T.B., Egebjerg, J., Watson, W.P., 2005. Changes in KCNQ2 immunoreactivity in the amygdala in two rat models of temporal lobe epilepsy. Brain Res. Mol. Brain Res. 141 (1), 66–73.
Pike, F.G., Goddard, R.S., Suckling, J.M., Ganter, P., Kasthuri, N., Paulsen, O., 2000. Distinct frequency preferences of different types of rat hippocampal neurones in response to oscillatory input currents. J. Physiol. 529 (1), 205–213.
Prescott, S.A. De, Koninck, Y., 2003. Gain control of firing rate by shunting inhibition: roles of synaptic noise and dendritic saturation. Proc. Natl. Acad. Sci. U. S. A. 100 (4), 2076–2081.
Racine, R.J., Mosher, M., Kairiss, E.W., 1988. The role of the pyriform cortex in the generation of interictal spikes in the kindled preparation. Brain Res. 454 (1–2), 251–263.
Sohal, V.S., Zhang, F., Yizhar, O., Deisseroth, K., 2009. Parvalbumin neurons and gamma rhythms enhance cortical circuit performance. Nature 459 (7247), 698–702.
Su, T., Cong, W.D., Long, Y.S., Luo, A.H., Sun, W.W., Deng, W.Y., Liao, W.P., 2008. Altered expression of voltage-gated potassium channel 4.2 and voltage-gated potassium channel 4-interacting protein, and changes in intracellular calcium levels following lithium-pilocarpine-induced status epilepticus. Neuroscience 157 (3), 566–576.
Suzuki, N., Bekkers, J.M., 2010. Inhibitory neurons in the anterior piriform cortex of the mouse: classification using molecular markers. J. Comp. Neurol. 518 (10), 1670–1687.
Vacher, H., Mohapatra, D.P., Trimmer, J.S., 2008. Localization and targeting of voltage-dependent ion channels in mammalian central neurons. Physiol. Rev. 88 (4), 1407–1447.
Zhang, L., Weiner, J.L., Valiante, T.A., Velumian, A.A., Watson, P.L., Jahromi, S.S., Schertzer, S., Pennefather, P., Carlen, P.L., 1994. Whole-cell recording of the Ca(2+)-dependent slow afterhyperpolarization in hippocampal neurones: effects of internally applied anions. Pflugers Arch. 426 (3–4), 247–253.